

AD-A098 045

NAVAL RESEARCH LAB WASHINGTON DC

F/G 20/9

CALCULATIONS OF BRILLOUIN BACKSCATTER IN LASER-PRODUCED PLASMAS--ETC(U)

APR 81 W M MANHEIMER, D G COLOMBANT

UNCLASSIFIED NRL-MR-4503

NL

1 OF 1
AU A
294044



END
DATE
FILMED
5-81
DTIC

AD A 098045

April 24, 1961

DTIC
ELECTED
APR 22 1961

SECURITY CLASSIFICATION OF THIS PAGE (When Data Entered)

9 REPORT DOCUMENTATION PAGE		READ INSTRUCTIONS BEFORE COMPLETING FORM
1. REPORT NUMBER NRL Memorandum Report	2. GOVT ACCESSION NO. AD-A098	3. RECIPIENT'S CATALOG NUMBER 045
4. TITLE (and Subtitle) CALCULATIONS OF BRILLOUIN BACKSCATTER IN LASER-PRODUCED PLASMAS		5. TYPE OF REPORT & PERIOD COVERED Interim report on a continuing NRL problem
7. AUTHOR(s) W.M. Manheimer and D.G. Colombant		6. PERFORMING ORG. REPORT NUMBER
9. PERFORMING ORGANIZATION NAME AND ADDRESS Naval Research Laboratory Washington, D.C. 20375		8. CONTRACT OR GRANT NUMBER(s) 11/14 April 81
11. CONTROLLING OFFICE NAME AND ADDRESS U.S. Department of Energy Washington, D.C. 20545		10. PROGRAM ELEMENT, PROJECT, TASK AREA & WORK UNIT NUMBERS 47-0859-0-1 (15) 34
14. MONITORING AGENCY NAME & ADDRESS (if different from Controlling Office) (14) NEL-MF-1503		12. REPORT DATE April 24, 1981
		13. NUMBER OF PAGES 33
		15. SECURITY CLASS. (of this report) UNCLASSIFIED
		15a. DECLASSIFICATION/DOWNGRADING SCHEDULE
16. DISTRIBUTION STATEMENT (of this Report) Approved for public release; distribution unlimited.		
17. DISTRIBUTION STATEMENT (of the abstract entered in Block 20, if different from Report)		
18. SUPPLEMENTARY NOTES		
19. KEY WORDS (Continue on reverse side if necessary and identify by block number) Laser fusion Brillouin backscatter Laser plasma		
20. ABSTRACT (Continue on reverse side if necessary and identify by block number) Brillouin backscatter is calculated in an inhomogeneous laser produced plasma. Equations for the spatial dependence of the incident reflected and sound wave are numerically integrated through the underdense plasma. Effects investigated are the stabilizing effects of ion heating or nonlinear sound wave dissipation, flow velocity magnitude and gradient, electron heating and broad band incident laser light. We find that the effect of velocity gradient and broad band light can be very important in reducing the backscatter.		

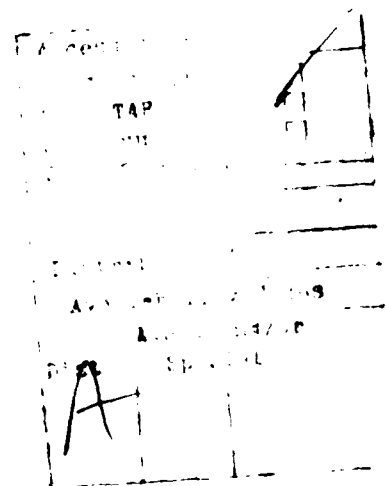
DD FORM 1 JAN 73 1473

EDITION OF 1 NOV 68 IS OBSOLETE
S/N 0102-014-6601

SECURITY CLASSIFICATION OF THIS PAGE (When Data Entered)

CONTENTS

I.	INTRODUCTION	1
II.	STIMULATED BRILLOUIN BACKSCATTER IN SUPERSONIC FLOW	3
III.	NONLINEAR THEORIES	6
IV.	CALCULATIONS IN SONIC AND SUBSONIC FLOW	12
V.	WIDE BAND INCIDENT LASER LIGHT	13
VI.	OTHER CALCULATIONS OF BRILLOUIN BACKSCATTER	14
	A. Dependence on Thermal Source and Resonant Position	14
	B. Reflection Where T_e Increases with Irradiance	15
	C. Calculations with Subsonic and Oscillating Velocity	16
	D. Backscatter for Single Structure Profiles	17
	E. A Broadband Pump	18
	F. Different Laser Wavelengths	18
VII.	SUGGESTIONS FOR FUTURE EXPERIMENTS	19
VIII.	CONCLUSIONS	20
	ACKNOWLEDGMENT	20
	REFERENCES	21



CALCULATIONS OF BRILLOUIN BACKSCATTER IN LASER-PRODUCED PLASMAS

I. INTRODUCTION

This paper studies Brillouin backscatter, which may be very important in laser fusion schemes in that it may reduce the amount of laser light available to couple to the pellet. This process has been studied experimentally for a long time.¹⁻¹² Experiments in which the plasma has a short scale length generally show that the fractional backscatter saturates as the irradiance increases. The plasma might have a short scale length because the laser pulse is very short, as is often the case in Nd laser produced plasmas,^{6,7} or because the focal spot is small (say less than 20 wavelengths) as is often characteristic of CO₂ laser produced plasmas.^{3,4,5} On the other hand long scale length plasma often show much more backscatter with no obvious tendency for saturation for reflection below 50 or 60%. One way to produce a long scale length plasma is to use a prepulse to produce a target plasma and then shoot the main laser beam into it. These experiments have been done at NRL^{8,9} recently and also elsewhere,¹⁰ using an Nd laser produced plasma. More recently, similar results were found with a CO₂ laser produced plasma.¹¹ Long scale length plasmas can also be produced by a gas jet.¹² These show Brillouin backscatter which saturates at 40 to 60%. Often in laser experiments, the fractional backscatter seems to be almost uncorrelated with any thing,^{6,7} that is graphs of fractional backscatter versus irradiance or some other parameter, show large scatter. One possible explanation¹³ is that very small prepulses, which might have been undetected in earlier experiments are responsible for the backscatter. This paper is motivated principally by experiments in which the backscatter seems to depend on the physical parameters in a fairly smooth and predictable way. In this respect the NRL prepulse experiments are particularly interesting because it measures the density profile of the prepulse plasma up to a density of about one-tenth critical.^{8,9} Specifically, it finds an exponential density fall off with a scale length of about 100

Manuscript submitted March 5, 1981

μ . The density profile is not measured above $0.1 n_{cr}$, but the scale length must be much shorter there.¹³

Our method of calculating the backscatter consists of numerically solving the equations for the spatial evolution of the amplitude of the laser pump wave, reflected wave and ion acoustic wave. This approach differs from other similar approaches¹⁴⁻¹⁶ in that we do not use a plasma slab with sharp boundaries. Instead, the gradients in all quantities are explicitly accounted for. The backscatter ends not at any artificial boundary, but rather when the plasma density gets so small that there is no further amplification of the reflected wave. Our numerical solutions can (and often do) follow the interaction for distances of hundreds of free space laser wavelengths. The other way to theoretically study Brillouin backscatter is particle simulations.^{12, 17, 18, 19} Recent simulations¹⁸ have in fact shown some aspects that our calculations show. The problem with these simulations is that they work best when studying the transient response to the backscatter over short distances. For instance a simulation of $10^4/\Omega_p$ (about 10^5 time steps) corresponds to only 5 pico-seconds for an Nd laser produced plasma. Clearly a simulation with length and time scales sufficiently long to achieve a steady state for a plasma with realistic parameters would be extremely expensive. Thus the type of calculations we do here appears to be a necessary link between studying the basic physics with particle simulations and interpreting real experiments, especially as the laser pulse length and plasma size increase.

Section II sets up the equations for mode amplitude and presents solutions assuming no other nonlinear effect except pump depletion. The importance of velocity gradient and electron temperature in determining backscatter is demonstrated. However the functional dependence of R (reflection) on I (irradiance) is very sharp. For instance a factor of 3 increase in I can increase R from 1% to 50%.

Section III examines whether nonlinear effects on the sound wave can slow down the dependence of R on I . There are two nonlinear effects we consider, an increase in the sound wave damping, and a limit on sound wave amplitude. As in Ref. 14, we find that an increase in dissipation has some effect

on reflection for either long or short gradient scale length plasmas. However this effect is less important than other physical effects which limit reflection. A limitation on sound wave amplitude however, does have some effect on the reflection for short scale length plasmas, but does not for long scale length plasmas. Thus a nonlinear limit on sound wave amplitude is thereby identified as one physical process which gives rise to saturation of R vs I curves for short scale length experiments.

Section IV presents another, much more economical way of calculating reflection which is uniformly valid if the sound wave is strongly damped, and gives the same total reflection in all cases. It can be incorporated in full simulation codes.

Section V presents calculations for a wide band laser pump. We show that, as discussed by others, a wideband pump can significantly reduce reflection.

Section VI presents a variety of calculations of Brillouin backscatter. Principally it again addresses the question of what slows down the increase of reflection with irradiance. One very important effect is the increase of electron temperature with irradiance. We find that this effect alone gives rough agreement with the NRL prepulse backscatter experiments. A combination of this effect and a nonlinear sound wave amplitude limitation appears to be responsible for the saturation of reflection with increasing irradiance for short pulse experiments. Also Section VI presents other calculations on backscatter with a wide band pump, with subsonic blowoff velocity and with spatially oscillating blowoff velocity.

Section VII suggests several experiments which can test the concepts developed in this paper, and finally Section VIII presents conclusions.

II. STIMULATED BRILLOUIN BACKSCATTER IN SUPERSONIC FLOW

The equations which describe stimulated Brillouin backscatter in a spatially varying medium are

$$\left[\frac{\partial}{\partial t} + v_s + \frac{\partial}{\partial x} v_s \right] A_s = \gamma_s A_p A_r^* \exp i \int^x (k_p - k_r - k_s) dx \quad (1a)$$

$$\left(\frac{\partial}{\partial t} + \nu_r + \frac{\partial}{\partial x} v_r \right) A_r = \gamma_0 A_p A_s^* \exp i \int^x (k_p - k_r - k_s) dx \quad (1b)$$

$$\left(\frac{\partial}{\partial t} + \nu_p + \frac{\partial}{\partial x} v_p \right) A_p = -\gamma_0 A_s A_r \exp i \int^x (k_p - k_r - k_s) dx \quad (1c)$$

where $|A^2|$ is the amplitude of the action density of the mode and A is taken to have the phase of the electric field E . That is:

$$A = A(x, t) \exp i \int k dx - \Omega t + c.c.$$

The indices p , r , and s denote the pump (incident) wave, reflected wave and sound wave at frequencies Ω_p , Ω_r and Ω_s , and the k 's are the wave numbers of the associated waves

$$k_p = \frac{1}{c} (\Omega_p^2 - \omega_p^2)^{1/2} \quad (2a)$$

$$k_r = \frac{1}{c} (\Omega_r^2 - \omega_p^2)^{1/2} \quad (2b)$$

$$k_s = \frac{\Omega_p - \Omega_r}{c_s + v} \quad (2c)$$

Here c_s is the sound speed assumed positive, v is the flow velocity and ω_p is the plasma frequency. Also v_s is the group velocity of the sound wave in the flow ($v_s = v + c_s$) and $v_{r,p}$ are the group velocities for the reflected and incident or pump light. In order for the matching conditions to be satisfied, $\Omega_r = \Omega_p - \Omega_s$.

The resonant point is defined as that point in the plasma $k_i = k_s + k_r$. For Brillouin backscatter $k_s \approx 2k_p$, $k_r \approx -k_p$. If the flow is supersonic toward the laser $c_s + v < 0$ so that backscattered light is blue shifted. The ν 's are the linear damping rates of the waves. For the incident and reflected light we use inverse bremsstrahlung

$$\nu_{p,r} = \frac{1}{2} \left(\frac{\omega_{pe}}{\Omega} \right)^2 n_p Z \ln \Lambda / 3.5 \times 10^5 T_e^{3/2}$$

while for the sound wave, we use the Landau damping rate

$$\nu_s = \sqrt{\frac{\pi}{8}} \frac{m}{M} \frac{\omega_i^4}{\omega_s^3 \left(1 + \frac{6k_s^2 T_i}{\omega_i^2 M} \right)} \left[1 + Z \sqrt{\frac{M}{m}} \left(\frac{T_e}{T_i} \right)^{3/2} \exp \left(-\frac{\omega_i^2 M}{2k_s^2 T_i} \right) \right] \quad (3)$$

with

$$\omega_l = \frac{\omega_{pi}}{\sqrt{2}} \left\{ 1 + \left[1 + 12(1 + k_s^2 \lambda_D^2) \frac{T_i}{T_e} \right]^{1/2} \right\}^{1/2} \frac{k_s \lambda_D}{1 + k_s^2 \lambda_D^2}^{1/2}, \quad \omega_s = k_s c_s$$

which is valid for $ZT_e \gg T_i$. Notice that ν_s is a rapidly increasing function for temperature. The

quantity A is related to the electric field through the standard relation $A^2 = \frac{\partial \epsilon}{\partial \omega} \frac{E^2}{8\pi}$, and

$$\gamma_o = \frac{\omega_{pi} e (M/Zm)^{1/4}}{m \Omega_i \sqrt{c v_e}} \left(\frac{2\pi \Omega_p}{1 + \frac{k_p^2 c^2}{\Omega_p^2}} \right)^{1/2}$$

Equations (11a, b) with $\nu = 0$ are the linear equations for Brillouin backscatter discussed by Rosenbluth.²⁰ If the flow is supersonic (that is v_r and v_s have the same sign) these equations predict spatial amplification of the backscattered wave and a steady state treatment is quite straightforward. The total amplification A_r between $\chi = -\infty$ and $\chi = +\infty$ is given by

$$\left| \frac{A_r(\infty)}{A_r(-\infty)} \right| = \exp \frac{\pi \gamma_o^2 A_i^2}{K v_r v_s} \quad (4)$$

where $2K = \frac{d}{dx}(k_p - k_r - k_s)$. If the flow is subsonic (that is v_r and v_s have opposite signs), Eq. (1a,

b) predict absolute instability in uniform bounded media. Rosenbluth et al.²¹ have shown that inhomogeneity changes the nature of the instability from absolute to convective. However the spatial and temporal behavior of the reflected wave is quite complex it is not apparent from Rosenbluth's work how one could do a steady state theory. In this section we consider only supersonic flow and deal with subsonic flow later. Equation (1c) includes the effect of pump depletion.

The basic procedure then is to numerically integrate Eqs. (1a, b, c) from somewhere below the critical surface toward the laser. The density profile is as measured in recent experiments on Brillouin backscatter with structured pulses.

$$n_e(x) = \begin{cases} n_{eo} \exp\left[-\frac{x}{l_1}\right] & n_e > 10^{20} \text{ cm}^{-3} \\ n_{eo} \exp\left[-\frac{(x-x_0)}{l_2}\right] & n_e \leq 10^{20} \text{ cm}^{-3} \end{cases} \quad (5)$$

with $l_1 = 20 \mu$, $l_2 = 100 \mu$ and x_0 the location where $n_e = 10^{20} \text{ cm}^{-3}$. We assume here a Nd laser produced plasma. These results can all be scaled to other laser wavelengths as will be discussed later. The resonant point is taken at $n_e = 0.12 n_{cr}$ the backscattered irradiance is taken as 10^{-8} times the incident irradiance. Later we will show that results are not very sensitive to these choices. Another important parameter to choose is the velocity profile. We study two choices

$$\begin{cases} v(x) = -\alpha c_s \\ v(x) = -c_s \left[1 + \frac{x_{cr} - x}{l_2} \right] \end{cases} \quad (6)$$

where x_{cr} is the location of the critical density and α is a parameter greater than 1. The former case has uniform velocity, the latter has a velocity gradient roughly equivalent to that of an isothermal rarefaction wave. For all cases, $ZT_e/T_i = 10$, $Z = 2.66$ (CH_2 target). Plots of power reflection versus incident irradiance for 1 micron laser light are shown in Fig. 1 for three choices of electron temperature, $T_e = 1 \text{ keV}$, 3 keV and 10 keV . For the choice of parameters (and also in all other calculations we do), the damping of the incident and reflected wave is negligible. Also shown in the dotted curve in Fig. 1 is the functional form of reflectance versus irradiance as predicted by Eq. (7) of Ref. 14 for the case of ν_i (ν_i in the notation of Ref. 14) equal to a constant. It is clear that the velocity gradient, increases by about an order of magnitude the irradiance required for a given reflection. Notice that in all cases, reflection increases very rapidly with irradiance with no tendency for saturation below about 70% reflectance. In the next sections we discuss physical mechanisms which could give rise to saturation.

III. NONLINEAR THEORIES

There has recently been discussion as to whether nonlinear effects on the sound wave can significantly limit the backscatter. There are basically two effects which are possible. First of all, there may be some nonlinear effect which limits the sound wave amplitude A_s ; and secondly, as the sound wave grows it heats the ions so that ν_i increases. In this section we study these effects.

We find that if A_s is limited, the backscatter depends crucially on what its phase is as it propagates away from the interaction region. There are at least two possibilities. If the damping ν_s , and coupling γ_o , are weak, it oscillates as a freely propagating sound wave so that $A_s \sim \text{constant}$. On the other hand, if the damping and coupling are strong, it oscillates as a driven oscillator $A_s \sim \exp i \int (k_p - k_r - k_s) dx$. For the former, the size of the interaction region is governed by the phase mismatch scale length as discussed by Rosenbluth.²⁰ For the latter, the size of the interaction region is governed by the dissipation.^{22, 23} The amazing thing is that for either case (in the linear theory) the total amplification of the backscattered wave is as given in Eq. (4). For strong damping, there is a weak interaction over an extended region; for weak damping there is a very localized strong interaction. Both give the same total amplification.

To show this, consider the ion wave equation in steady state and neglect the variation in v_s . Assuming A_r is constant so the term on the right drives a strongly damped oscillator, we find

$$A_s = \frac{\frac{\gamma_o}{v_s} A_p A_r^* \exp i \int (k_p - k_r - k_s) dx}{i(k_p - k_r - k_s) + \nu_s/v_s} \quad (7)$$

Inserting this into the equation for A_r and taking only the real part, assuming $\nu_r = \frac{d\nu_r}{dx} = 0$, we find

$$\frac{d}{dx} |A_r|^2 = \frac{\frac{2\gamma_o^2}{v_r v_s} |A_p|^2 |A_r|^2 \frac{\nu_s}{v_s}}{(k_p - k_r - k_s)^2 + (\nu/v_s)^2} \quad (8)$$

Integrating Eq. (8) we find that the total amplification is as given in Eq. (4) independent of ν_s . The width of the resonant region now is given roughly by ν_s/kv_s so as ν_s increases, the resonant region broadens. Thus according to linear theory, the amplification is the same for $\nu_s \approx 0$ as it is for large ν_s , so that the actual amplification should be very nearly independent of ν_s . In contrast, for a homogeneous slab, of width L the spatial growth rate is proportional to ν_s^{-1} . Thus the number of e foldings (in the linear regime) is proportional to $\frac{A_p^2 L}{\nu_s}$.

Any nonlinear theory which relies on an increase in ν_s must account for a broadening of the resonant region also. Of course the problem is much more complicated than indicated here because (a) as ν_s increases, the resonant region ultimately can become larger than the plasma, (b) pump depletion occurs and (c) variation in other quantities besides wave number mismatch must also be accounted for. Our calculations show that there is some reduction in backscatter resulting from an increase in ν_s . However this effect seems less than the effect of increasing the velocity gradient or electron temperature.

Next we consider the effect of a limit on the amplitude of the second wave. Let us assume that in addition to an increase in ν_s , a nonlinear effect, for instance ion trapping, actually does more, and somehow clamps a limit on the sound wave amplitude. Whether this is an important effect or not then depends on how large an amplitude the sound wave would achieve if there were no limit. The shorter the scale length, the larger the sound wave amplitude must be to cause a given reflection. Thus we expect a limit on sound wave amplitude to play a larger role for short scale length (i.e., short pulse experiments) than for long scale length or double structure (i.e., long or double structured laser pulses).

The last possibility we consider is that the sound wave amplitude be limited, but there be no increase in ν_s . Thus the wave propagates like a freely propagating sound wave. Since the interaction now weakens, but without a corresponding increase in interaction length, the backscatter can be severely limited in this case.

We examine two approaches to increases ν_s . The first is just a straight increase of this quantity. The solid curves show in Fig. 2 reflection versus irradiance for four choices, $ZT_e/T_i = 10$, $ZT_e/T_i = 6$, $\nu_s = \omega_e/2$ and $\nu_s = \omega_e$. The ratio of irradiance needed for given reflection in these cases are roughly 1:2:3:4 so that ion heating can give rise to some reduction in backscatter. If the ion heating is so intense that $\nu_s \sim \omega_e$ ($ZT_e \sim T_i$) there can be a fairly significant reduction, although it is still less than either the effect of a velocity gradient or what the effect would be for a homogeneous slab. For

instance if $Z_e T/T_i = 10$, then ν_s/ω_s is about 0.015. In a homogeneous slab, an increase of ν_s from this to $\nu_s/\omega_s = 1$ would imply that for the same reflection, the irradiance would have to be about sixty times greater. However for the inhomogeneous plasma, the irradiance is only about 4 times greater, so the effect of an increase of ν_s is much less than it would be for a homogeneous slab.

Another approach to the problem of an increase in ν_s is to postulate some nonlinear dissipation of the sound wave. Thus ν_s will be some increasing function of A_s . We use a model based on ion trapping. The idea here is that as the wave sound grows it traps ions and forms a non-thermal ion tail to the distribution function. This non-thermal tail Landau damps the wave. The temperature of this tail is taken to be the ion mass times the square of the wave phase velocity or roughly ZT_e . Once the number of ions in the tail is known, the Landau damping rate can be calculated. If the trapping width is $\Delta v = 2\sqrt{\frac{Ze\phi}{M}}$, where ϕ is the amplitude of the electrostatic potential fluctuation, the number of ions in the tail is $\int_{v_p - \Delta v}^{v_p + \Delta v} f_i(v) dv$ where v_p is the wave phase velocity. We now calculate the number of ions in the tail of a Maxwellian at temperature ZT_e . Doing the calculation in the same way from $(v_p - \Delta v)$ to ∞ , the number of ions is

$$n_t = n \left[\frac{\operatorname{erf}\left(\frac{v_p + \Delta v}{(2T_e/M)^{1/2}}\right) - \operatorname{erf}\left(\frac{v_p - \Delta v}{(2T_e/M)^{1/2}}\right)}{\operatorname{erfc}\left(\frac{v_p - \Delta v}{(2ZT_e/M)^{1/2}}\right)} \right] \quad (9)$$

and the damping rate from this tail would be

$$\nu_{ST} = \sqrt{\frac{\pi}{8}} \frac{m}{M} \frac{\omega_i^4}{\omega_s^3(1 + 6k_y^2 T_e/\omega_i^2 M)} \left\{ 1 + Z \left(\frac{M}{m} \right)^{1/2} \frac{n_t}{n} \exp - 1/2 \right\} \quad (10)$$

with ω_i defined in Eq. (3c). Thus, as Δv increases, the damping rate also increases. We have computed the reflection for $ZT_e/T_i = 10$, $T_e = 3$ keV using Eq. (10) or Eq. (3c), whichever is larger, for ν_s . The results are shown in Fig. (2), the dotted curve being for anomalous ν_s for the case of a double structured profile with a velocity gradient. There is very little reduction in backscatter. Although the backscatter is not significantly reduced, an examination of the detailed structure of say A , shows that the interaction region is now much larger, and that in large regions of the $\nu_s/k, c_s \leq 1$.

Finally let us note that this change in the character of the interaction as ν_s increase has been observed also in particle in cell simulations.¹⁸ When an ion tail is generated by the ion acoustic wave, the strength of the interaction decreases and there is a transition from what Kindel calls coherent to diffuse scattering.

The work of Ref. (14) does find saturation by increasing ν_s . However this work uses a slab model with sharp boundaries. The width of the slab is independent of ν_s , so there is no chance for the interaction length to increase as ν_s increases. We find, on the contrary, that the gradients and associated phase mismatch, play a very important role, even far above threshold.

Let us now consider the second possibility, namely that there is an increase in dissipation coupled with a maximum value of $\frac{e\phi}{T_e}$. One reason for such a limit is that as $\frac{e\phi}{T}$ tries to grow, it not only Landau damps on ions in the tail, but it must also drag more ions into the tail. This could limit the amplitude of $\left(\frac{e\phi}{T_e}\right)$.²⁴ We use the same model for the anomalous dissipation, but now, in the equations for A_r and A_s , we do not allow $\frac{e\phi}{T_e}$ to be larger than 0.05. The result for R versus I is shown as the dashed curve in Fig. 2. Note that the reduction in reflection is very slight. The reason is that with the strong dissipation, $\frac{e\phi}{T_e}$ does not get much above 0.05 even without the limit.

We now consider the third possibility, namely that as the ion wave traps ion, it forms a coherent phase space vortex structure so that it moves as a freely propagating ion wave (perhaps with a nonlinear frequency shift²⁵). A model for this is to limit the ion wave to some maximum amplitude but not to increase the dissipation. Thus the interaction region does not increase and if it is small to begin with, the reflection significantly decreases. In Fig. 2, the dash-dot curves show reflection as a function of irradiance for maximum density fluctuations of $\frac{e\phi}{T} = 0.05$ and $\frac{e\phi}{T_e} = 0.1$. There is now a significant reduction in reflection and saturation with irradiance.

However it seems unlikely to us that the interaction could be coherent for very long. The ion wave would almost surely break, and the trapped ions would randomize, leading to Landau damping. This, in fact, is what has been observed in recent simulations.¹⁸ Also, if the interaction region is small, there is virtually no ray-retrace in the backscattered wave since it requires a long distance to set up the volume hologram.^{26,27} Since at least some ray-retrace is a feature of the experiments, a freely propagating ion wave with coherently trapped ions does not seem to be a viable nonlinear state.

The next question is whether by shortening the plasma length, it is possible to achieve saturation of the reflection. We have examined this for a plasma with an exponential profile with a density gradient scale length as short as 15μ . Using the dissipation model of Eq. (10), we find only very slight change in the shape of the R versus l curve even though $\nu_s/k_s c_s \geq 1$ for most of the plasma. Thus a nonlinear dissipation alone has very little effect on the backscatter. However, an $\frac{e\phi}{T_e}$ limit, coupled with an anomalous dissipation does have a significant effect on the backscatter for short scale length plasmas. In Fig. 3 we show R versus l curves for a 30μ scale length plasma with a velocity profile given by

$$v = -c_s (x = x_{cr}) \left[1 + \frac{x_{cr} - x}{l} \right] \quad (11)$$

with

$$l = 30 \mu.$$

The solid curve is the result for no anomalous dissipation, the dashed curve is for anomalous ν_s , and the dotted curve is for ν_s given by Eq. (10) but also with an $\frac{e\phi}{T_e}$ limit of 0.05. This latter curve does not show saturation, but does show a much slower increase of R with l . The reason is that in the short plasma we consider here, much larger values of $\frac{e\phi}{T_e}$ than in the longer plasma are needed to produce the same reflection. In Section VI we will see that if the variation of T_e with l is accounted for, the increase of R with l is much slower still, so that saturation should result.

IV. CALCULATIONS IN SONIC AND SUBSONIC FLOW

Calculations with Eqs. (1 a-c) for sonic and subsonic flow are much more difficult because (a) the equations are singular at the sonic point and (b), for purely subsonic flow the reflected and ion acoustic waves are at their thermal levels at different points in the plasma so one cannot easily calculate the reflection with a single integration through the plasma. However, the calculation can be made for sonic and subsonic flow if one uses Eq. (7) for A_s and then derives equations like Eq. (8) for $|A_r|^2$ and $|A_p|^2$. The resulting equations are quite straightforward and are

$$\begin{aligned} v_p \frac{d}{dx} |A_p|^2 + 2|A_p|^2 \frac{dv_p}{dx} + 2\nu_p |A_p|^2 = -v_r \frac{d}{dx} |A_r|^2 - 2|A_r|^2 \frac{dv_r}{dx} - 2\nu_r |A_r|^2 \\ = \frac{-2\gamma_o^2 |A_p|^2 |A_r|^2 \nu_s / v_s^2}{(k_p - k_r - k_s)^2 + (\nu_s / v_s)^2} \end{aligned} \quad (12)$$

Equation (12) are quite straightforward. They are two real equations and can be integrated from the critical surface outward to calculate the reflection. They are valid everywhere if the ion wave is strongly damped. If the ion wave is weakly damped, they give the same total amplification as Eqs. (1 a-c) for supersonic flow.

Notice that Eq. (12) depends only on v_s^2 so it gives the same amplification for positive and negative v_s . Thus it can be used where v_r and v_s have opposite sign (subsonic flow) and it gives the same amplification as found in Refs. 20 and 21. Also the equation is no longer singular at $v_s = 0$. If the velocity is subsonic near the critical surface and increases uniformly through a sonic point, so that it is supersonic at lower densities, resonant positions with $\Omega_s > 0$ (ω being the doppler shifted sound wave frequency) will be in the subsonic plasma, while resonant positions with $\Omega_s < 0$ will be in the supersonic plasma. If $\omega = 0$, then $k_s = \infty$ at the sonic point so that a sound wave in the supersonic plasma cannot propagate into the subsonic plasma and vice versa. Thus for a plasma with a sonic transition, the procedure for red shifted light is to start the integration of Eq. (12) at the critical surface and march outward until the sonic point and then stop. For blue shifted light the procedure is to start at the sonic point and integrate outward into the supersonic plasma.

We have compared results for numerical integration of Eq. (12) with results for numerical integration of Eqs. (1a-c) for both strong and weak damping. In all cases, graphs of reflection versus irradiance were quite close to each other and had basically the form shown in Fig. 1. However, the detailed spatial structure say A_r can be quite different depending on whether the damping is strong or weak. Finally let us note that numerical integration of Eq. (12) is so economical that it can easily be incorporated in a full one dimensional fluid simulation.

V. WIDE BAND INCIDENT LASER LIGHT

The equations developed in the previous section can also be applied to steady state, nonlinear calculations if the laser light has nonzero frequency bandwidth. For instance say there is a single reflected wave, but different incident waves so that the subscript p (on say Ω_p) now becomes an index of summation. Thus the equations for the frequency components of a wide-band incident laser source are

$$\begin{aligned} v_r \frac{d}{dx} |A_r|^2 + 2|A_r|^2 \frac{dv_r}{dx} + 2\nu_r |A_r|^2 &= - \sum_p \frac{2\gamma_0^2 |A_p|^2 |A_r|^2 \nu_s / v_s^2}{(k_p - k_r - k_s)^2 + (\nu_s / v_s)^2} a \\ \nu_p \frac{d}{dx} |A_p|^2 + 2|A_p|^2 \frac{d\nu_p}{dx} + 2\nu_p |A_p|^2 &= \frac{2\gamma_0^2 |A_p|^2 |A_r|^2 \nu / v_s^2}{(k_p - k_r - k_s)^2 + (\nu_s / v_s)^2} \end{aligned} \quad (13)$$

The reflected wave frequency Ω_r is specified and there are now different pump wave frequencies Ω_p . The sound wave frequency for each pump wave is given by $\Omega_r - \Omega_p$. Given these frequencies, each wave number is determined by Eqs. (2a-c). For each pump wave, there will be a resonant location in the plasma where $k_p(x) = k_r(x) + k_s(x)$.

If the laser irradiance in the plasma is given, then $\sum_p |A_p(\Omega)|^2$ is determined. However if there is a broad spread in frequencies it is possible that only a very small portion of the incident spectrum resonant with any reflected wave in the underdense plasma. Thus the backscatter can be significantly reduced with a broad band pump. This is analogous to the reduction in linear growth rate of the Brillouin backscatter instability in homogeneous media, by a broadband pump.²⁸ As a rule of thumb, one can calculate the bandwidth necessary to reduce the backscatter in an experiment as follows. Assume that for coherent incident light, the backscattered light has bandwidth $\delta\omega$. If this $\delta\omega$ measures the

spread in resonant positions for the scattering, then a wide band pump should have bandwidth $\Delta\omega \gg \delta\omega$ to significantly reduce the backscatter.

VI. OTHER CALCULATIONS OF BRILLOUIN BACKSCATTER

In this section we present the results of other calculations of reflectivity. Since most graphs of reflection coefficient versus irradiance have the same form as those shown in Figs. 1 and 2, instead of plotting the graphs themselves, we simply give a single point to them.

The graphs themselves can be easily constructed then. For most of our calculations, we have used Eqs. (1a-c). However, for calculations with subsonic flow a broadband pump and flow with a spatially oscillating velocity, we used Eq. (12). Unless otherwise specified $ZT_e/T_i = 10$, the density profile is as given in Eq. (4) and the velocity profile is either as given in Eqs. (5a or b). All calculations assume a Nd laser produced plasma. Unless otherwise specified $n_{cr} = 0.12 n_c$.

A. Dependence on Thermal Source and Resonant Position

For nearly all our calculations the irradiance of the reflected wave at the critical density is smaller than that of the incident wave by a factor of 10^{-8} . To test the dependence on this parameter, we have redone the calculation taking the reflected irradiance smaller by 10^{-4} for the case where the velocity is given by Eq. (5). We find that the reflection coefficient is 0.26% at an irradiance of 2.33×10^{15} W/cm² so that a change of 4 orders of magnitude in reflected irradiance changes the reflectivity by less than a factor of two along the horizontal axis.

Next we have examined the dependence of reflection on position of the resonant point. We have redone the calculations with resonant positions at $n = 0.2 n_c$, $0.12 n_c$, $0.08 n_c$ and with velocity gradient. The reflection coefficients are respectively 10% at an irradiance of 1.35×10^{15} W/cm², 19% at 2.9×10^{15} W/cm² and 20% at 3.5×10^{15} W/cm². In addition, we have calculated the reflection coefficient where all four reflected waves and their associated sound waves are simultaneously in the system (but where the initial irradiance of each reflected wave is smaller by a factor of 4) and where

there is no velocity gradient. The reflection is 30% at an irradiance of 4.2×10^{14} W/cm², which is nearly the same as for the single wave resonant at $n_r = 0.12 n_c$ and for no velocity gradient. Thus the reflection depends very weakly on both the resonant position and also on whether there is a single backscattered wave or a spectrum of waves resonant at different positions.

If there is a spectrum of backscattered waves, each resonant position corresponds to a different frequency. Thus a measurement of the backscattered spectrum, especially if it is time resolved, can give information on the flow velocities in the blow-off plasma.

B. Reflection Where T_e Increases with Irradiance

The curves in Fig. 1 show that reflection increases very rapidly with irradiance at fixed temperature. This rapid increase is usually not observed experimentally. One explanation is that the temperature does not remain fixed as the irradiance varies, but rather increases in some way with irradiance. We consider two possible scaling laws, $T_e \propto I^{1/3}$, and $T_e \propto I^{2/3}$ which cover those generally assumed. Plots of reflection versus irradiance for the two scaling laws without a velocity gradient are shown in Fig. 4. Figure 5 is an analogous plot with a velocity gradient. In the former case, T_e is assumed to be 1 keV at an irradiance of 8×10^{13} W/cm² and in the latter, 3 keV at 2×10^{13} W/cm². If $T_e \propto I^{1/3}$, there is some weakening of the dependence of R on I . For $T_e \propto I^{2/3}$, there appears to be a saturation in the reflection at around 40 to 60 percent at least over the range in irradiance indicated. According to linear theory, the reflection is constant if I/T_e is constant. Thus increasing T_e can greatly reduce the backscatter at given irradiance.

Also shown on Fig. 5 are measurements of reflection versus irradiance taken from Fig. 3 of Ref. 9. In Ref. 9, the density profile is roughly what we have assumed. Although the velocity profile is not measured, our choice of an isothermal rarefaction wave is certainly reasonable. We recall from Section III that for a long scale length experiment, a limit on sound wave amplitude had only a small effect on the reflection. However, the agreement between experiment and theory here is fairly good, so that the

increase in electron temperature with irradiance is probably responsible for slowing down the increase of R with I .

For short pulse experiments, as shown in Section III, a limit on the sound wave amplitude does have a strong effect on the functional dependence of reflection on irradiance. It seems reasonable then that a limit on sound wave amplitude, coupled with an increase in T_e with I can give rise to a saturation in reflection versus irradiance in short pulse experiments.

C. Calculations with Subsonic and Oscillating Velocity

Calculations of reflection as a function of irradiance were also made for subsonic flow with a flow velocity given by

$$\begin{cases} v = -0.3 c_s (x - x_{cr}) \left[1 + \frac{x_{cr} - x}{l} \right] & l = 100 \mu \\ v = 0. \end{cases} \quad (14)$$

We found reflection of 9% at an irradiance of $3.3 \times 10^{14} \text{ W/cm}^2$ for the former, and reflection of 9% at an irradiance of $7 \times 10^{14} \text{ W/cm}^2$ for the latter. Notice that the reflection is generally larger for subsonic flow. This could be one explanation for the fact that Brillouin backscattered light is experimentally observed to be red shifted about as often as blue shifted even though the flow is generally thought to be supersonic. That is while the flow is subsonic, stimulated Brillouin backscatter is enhanced.

Since velocity gradient is such a strongly stabilizing effect on stimulated Brillouin backscatter, it seems likely that one could reduce the backscatter by decreasing the velocity gradient scale length. One way to do this without significantly changing the flow-off plasma profile is to superimpose an oscillating velocity on the plasma. This could be achieved by oscillating the laser intensity. The backscatter can be significantly reduced for subsonic flow but only if the amplitude and wavelength of the velocity modulation are carefully chosen. If the wavelength of the velocity modulation is too long, there is almost no effect on the backscatter. Similarly, if the wavelength is too short there is also almost no

effect; presumably because, as the wave amplifies, it averages over the rapid oscillations. For the density profile given in Eq. (5), we find the optimum wavelength for the velocity modulation is about 50μ . Specifically, choosing the velocity profile

$$v = -0.3 c_s \left[1 + \frac{x_{cr} - x}{l} \right] + v_f \sin \left[-\frac{2\pi}{\lambda_f} x \right] \quad (15)$$

with $v_f = 10^7$ we find a reflection of 10% at $2.4 \times 10^{15} \text{ W/cm}^2$. Thus an optimum velocity modulation can increase the irradiance for given reflection by nearly an order of magnitude. However the backscatter for the oscillating velocity is still no less than backscatter for the supersonic flow profile we have examined.

D. Backscatter for Single Structure Profiles

It is of interest also to calculate backscatter from single structure plasma as this might be the case for laser fusion pellets. Therefore we consider a density profile

$$n_e(x) = n_{cr} \exp \left[-\frac{x}{l} \right] \quad (16)$$

and a velocity profile of either

$$v = -c_s (x - x_{cr}) \left[1 + \frac{x_{cr} - x}{l} \right] \quad (17a)$$

$$v = -\alpha c_s (x - x_{cr}) \text{ with } \alpha > 1. \quad (17b)$$

The former is an isothermal rarefaction wave, the latter has the velocity gradients artificially suppressed. Generally we feel that the higher the irradiance, the shorter the pulse, so we have let T_e vary with I . Values of T_e for various I 's are shown in Table 1.

In Fig. (6) are shown solid and dotted curves. They show the irradiance at which the reflection is 50% as a function of l for $ZT_e/T_i = 10$ with and without velocity gradient. We have also plotted as squares the irradiance of 50% reflection for $l = 30 \mu$ for $T_e = 6.6 \text{ keV}$ and 15 keV . A 50% increase in electron temperature has a fairly large effect on the backscatter. We have also attempted to examine the effect of an oscillating velocity. However, for the supersonic flow profiles examined here, there did not appear to be any significant reduction in backscatter.

E. A Broadband Pump

Here we examine Brillouin backscatter for broadband pump. The density and velocity gradients are as given in Eqs. (4) and (5) and the electron temperature is $T_e = 3$ keV and $ZT_e/T_i = 10$. The incident spectrum consists of 5 or 9 waves of equal amplitude and equal frequency spread. The center wave always has a resonant position at $n = 0.12 n_{cr}$. In Fig. 7 are shown the incident total irradiance for 10% reflection and 50% reflection as a function of bandwidth $\Delta\Omega_p/\Omega_p$. Here $\Delta\Omega_p$ is defined as the frequency spread between the center frequency and maximum (or minimum) frequency. Note that as $\Delta\Omega_p$ increases, the initial tendency is for the backscatter to slightly increase. The reason, apparently, is that as the resonant positions move away from each other the reflected wave is resonant with the incident spectrum over a large region, but not as strongly with any wave, in such a way that the net interaction increases. However as the bandwidth continues to increase, the reflection begins to decrease quite substantially. The reason is that as $\Delta\Omega$ increases, the different resonant positions move out of the underdense plasma so that the backscattered wave interacts with less and less of the incident spectrum.

F. Different Laser Wavelengths

If collisional damping of the incident and backscattered wave is neglected, all equations we have used are invariant to the scaling

$$\begin{aligned}
 L &\rightarrow \alpha L \\
 v &\rightarrow v \\
 \omega &\rightarrow \omega/\alpha \\
 n &\rightarrow n/\alpha^2 \\
 I &\rightarrow I/\alpha^2.
 \end{aligned}
 \tag{18}$$

This allows one to scale the results presented here to different laser wavelengths. However when scaling to shorter wavelengths, collisional effects become more and more important, so that the reflection coefficients should be progressively smaller than predicted by the scaling law in Eq. (18) as the wavelength decreases.

VII. SUGGESTIONS FOR FUTURE EXPERIMENTS

This work indicates that one of the most important quantities to determine in the blowoff plasma is the velocity and velocity gradient. It might be possible to measure this quantity experimentally by inserting in the outer edge of the laser target, a thin layer of high Z material which would line radiate at some frequency. This transition line would be frequency broadened by the ion temperature and frequency shifted by the plasma flow. The shift would be most visible if looked at head-on, but the broadening would be equally visible from all angles.

When the laser light reached this material, it would accelerate outward. The idea then would be to get a time resolved measurement of the Doppler shift of a transition line looking head-on from the time it first appears until it disappears. This would give the velocity as a function of time, and integrating, would give the velocity as a function of space. It is also important to note that the temporal motion of interferometry fringes does not give information about the flow velocity, but rather about the motion of the constant density surfaces. The two are essentially unrelated in laser produced plasmas. Kruer¹⁴ and others¹⁵ suggest that Brillouin backscatter gives rise to strong ion heating so that ultimately $ZT_e \sim T_i$. It would certainly be very interesting to attempt to measure the ion temperature in an underdense plasma in which Brillouin backscatter takes place. There appear to be two possible approaches to this problem, both of which could indicate ion temperature and possibly even detect the difference between heating the tail and body of the ion distribution function. The first is a variant of the method we have just discussed, namely seeding an outer layer of target with a high Z impurity, only now examining the Doppler broadening rather than Doppler shift of the associated line radiation.

The second technique, which we have proposed previously,²⁹ is to seed the outer part of the target with DT or $D-H_e^3$ and look for fusion neutrons or protons for the case where there is strong Brillouin backscatter. The number of 14 MeV neutrons or protons produced depends strongly on the ion temperature and Ref. 29 calculated it for Maxwellian ions. It should also be possible to calculate the neutrons or protons produced for an ion distribution with a non-thermal tail. Since the production of

fusion neutrons is most likely more sensitive to non-thermal tails on the ion distribution function, and the Doppler broadening of line radiation probably most sensitive to the bulk temperature, a comparison of the two measurements might indicate whether the ion distribution function is or is not thermal.

VIII. CONCLUSIONS

We have presented here a large number of calculations of Brillouin backscatter in laser produced plasmas. We find that at given irradiance, the backscatter depends quite strongly on velocity, velocity gradient and electron temperature. It depends more weakly on ion temperature or other anomalous dissipation. For a short scale length plasma, the backscatter can be reduced by a nonlinear limit on the amplitude of the sound wave. However this effect becomes less and less important as the scale length increases. The saturation of backscatter with irradiance characteristic of short pulse experiments seems to be a combination of saturation by $\frac{e\phi}{T_e}$ limit as discussed in Section III and increase of T_e with irradiance as discussed in Section VI. The lack of saturation with irradiance in double pulse experiments results from the fact that an $\frac{e\phi}{T_e}$ limit no longer plays an important role.

All our studies were done for Nd-laser produced plasma. However as long as collisional damping of the incident and reflected light is not important, the calculations scale easily to any wavelength. The two principal methods available to reduce the backscatter seem to be in control of the blow-off velocity (possibly including setting up a spatially oscillating velocity), and increasing the bandwidth of the incident light.

ACKNOWLEDGMENT

We would like to thank Drs. B. Ripin, R. Lehmborg, M. Herbst and S. Bodner for a number of useful discussions. This work was supported by the Department of Energy.

REFERENCES

1. B.H. Ripin, J.M. McMahon, E.A. McLean, W.M. Manheimer, and J.A. Stamper, Phys. Rev. Lett. 33, 634 (1974)
2. L.M. Goldman, J. Soures and M.J. Lubin, Phys. Rev. Lett. 31, 1184 (1973)
3. K.B. Mitchell, T.F. Stratton and P.B. Weiss, App. Phys. Lett. 27, 11 (1975)
4. B. Grek, H. Pepin, T.W. Johnston, J.N. Leboeuf, and H.A. Baldis, Nucl. Fusion 17, 6 (1977)
5. B. Grek, H. Pepin, F. Rheault, Phys. Rev. Lett. 38, 898 (1977)
6. M.D. Rosen, D.W. Phillion, V.C. Rupert, W.C. Mead, W.L. Kruer, J.J. Thomson, H.N. Kornblum, V.W. Slivinsky, G.J. Caporaso, M.J. Boyle, and K.G. Tirsell, Phys. Fluids 22, 2020 (1979)
7. R.H. Haas, W.C. Mead, W.L. Kruer, D.W. Phillion, H.N. Kornblum, J.D. Lindl, D. Mac Quigg, V.C. Rupert, and K.G. Tirsell, Phys. Fluids 20, 322 (1977)
8. B.H. Ripin, F.C. Young, J.A. Stamper, C.M. Armstrong, R. Decoste, E.A. McLean, and S.E. Bodner, Phys. Rev. Lett. 39, 611 (1977)
9. B.H. Ripin and E.A. McLean, Appl. Phys. Lett. 34, 809 (1977)
10. R.E. Turner and L.M. Goldman, Phys. Rev. Lett. 44, 400 (1980)
11. R. Decoste, P. Lavigne, H. Pepin, G. Mitchell, and F. Martin, Bull. Am. Phys. Soc. 25, 856 (1980)
12. F.J. Mayer, G.E. Busch, C.M. Kinzer and K.G. Estabrook, Phys. Rev. Lett. 44, 1498 (1980)
13. B.H. Ripin, private communication.
14. W.L. Kruer, Phys. Fluids, 23, 1273 (1980)

MANHEIMER AND COLOMBANT

15. T. Speziale, J.F. McGrath and R.L. Berger, *Phys. Fluids* **23**, 1275 (1980)
16. D.W. Phillion, W.L. Kruer and V.C. Rupert, *Phys. Rev. Lett.* **39**, 1529 (1977)
17. D.W. Forslund, J.M. Kindel and E.L. Lindman, *Phys. Fluids* **18**, 1017 (1975)
18. J.M. Kindel, presented at *IEEE Conference on Plasma Science*, Madison, Wis., Apr. 1980
19. W.L. Kruer, K. Estabrook and K.N. Sinz, *Nucl. Fusion* **13**, 952, (1973)
20. M.N. Rosenbluth, *Phys. Rev. Lett.* **29**, 565 (1972)
21. M.N. Rosenbluth, R.P. White and C.S. Liu, *Phys. Rev. Lett.* **31**, 1190 (1973)
22. K. Nishikawa and C.S. Liu in *Advances in Plasma Physics* (Wiley, New York, 1976 Vol. 6, p. 3)
23. A.N. Kaufman and B.I. Cohen, *Phys. Rev. Lett.* **30**, 1306 (1973)
24. W. Manheimer and R. Flynn, *Phys. Fluids* **17**, 409 (1974)
25. W. Manheimer and R. Flynn, *Phys. Fluids* **14**, 2393 (1971)
26. R.H. Lehmberg, *Phys. Rev. Lett.* **41**, 863 (1978)
27. R.H. Lehmberg and K.A. Holder, to be published, also *NRL Memorandum* 4192, April 1980
28. J.J. Thomson, *Nucl. Fusion* **15**, 2012 (1975)
29. D.G. Colombant and W.M. Manheimer, *Phys. Fluids* **23**, 2512 (1980)

Table 1 — The Density Gradient
Scale Length at the
Assumed Electron Temperatures

I_a	T_e keV
30	10
100	5
300	3
1000	1

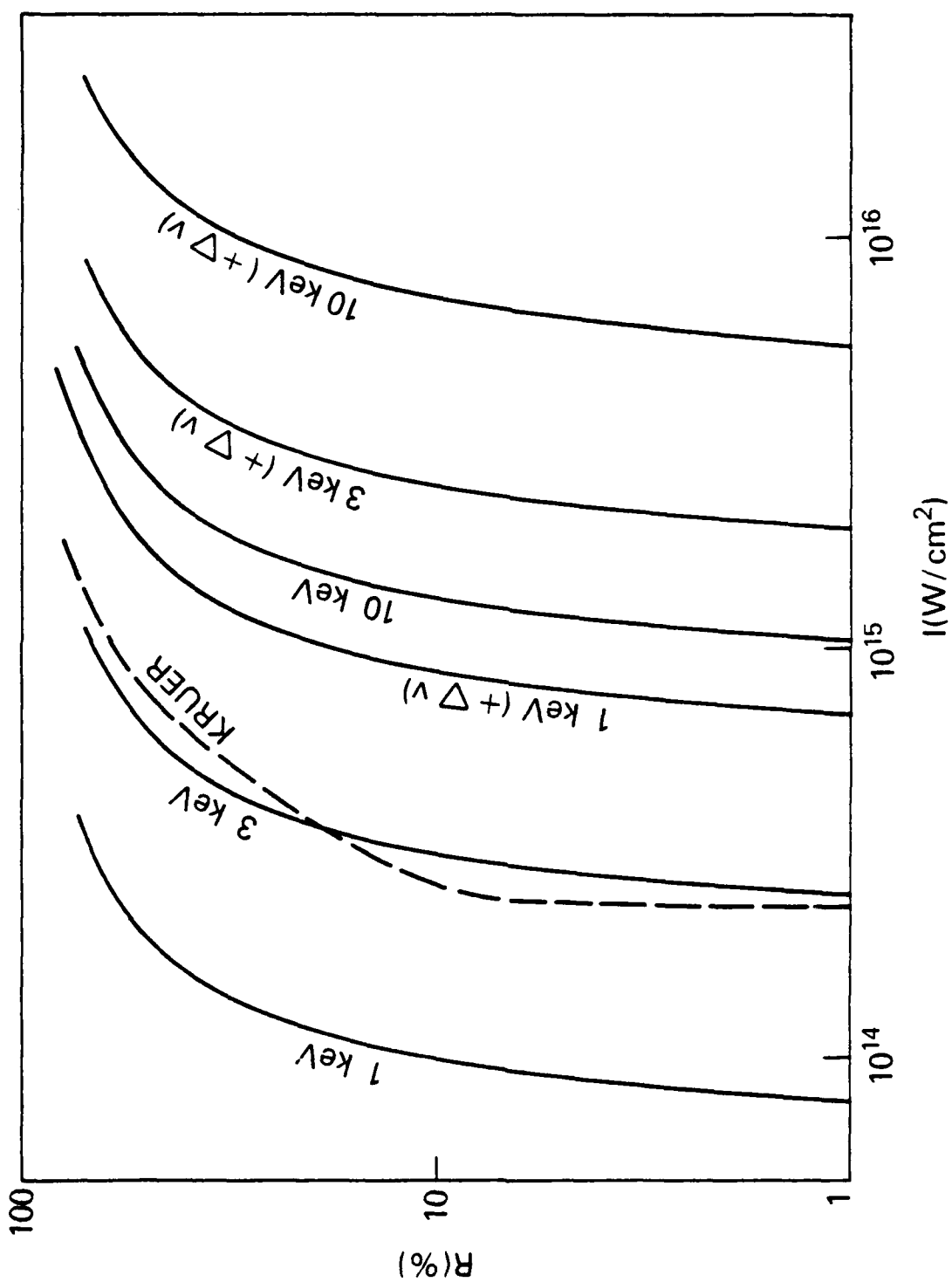


Fig. 1 — Double structured density profile: solid curves, plots of R versus I for three different electron temperatures with and without velocity gradient; dashed curve, plot of R versus I from Eq. (7) of Ref. 14

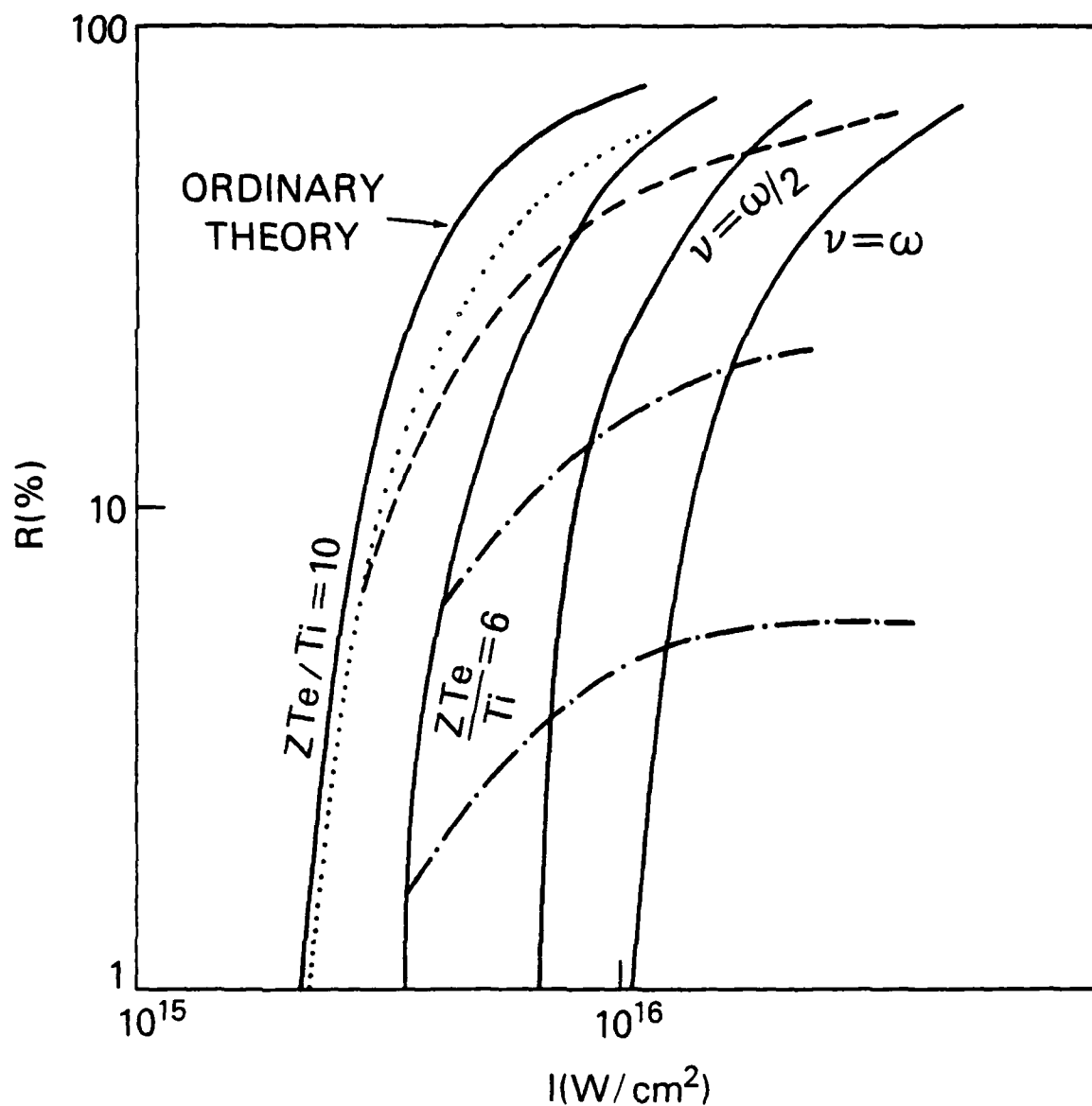


Fig. 2 — Double structured density profile, solid curves, R versus I for $ZT_e/T_i = 10$ and 6, $\nu/\omega = 1.2$ and 1; dotted curve, R versus I with anomalous dissipation; dashed curves R versus I for anomalous dissipation and $\frac{v\phi}{T} < 0.05$; dashed-dot curves, R versus I for $\frac{v\phi}{T} < 0.05$ or 0.1 but with no dissipation

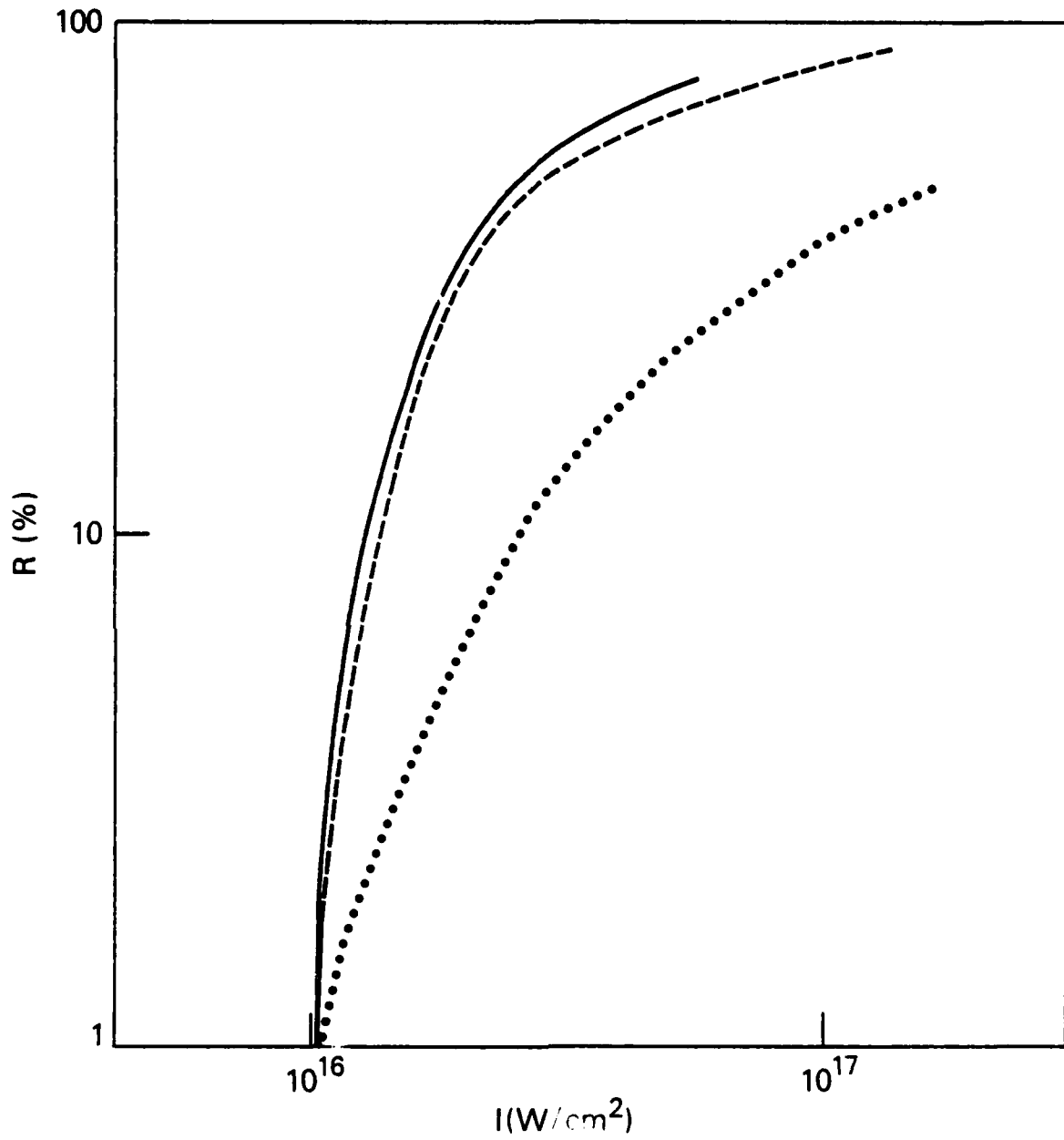


Fig. 3 — Single structure density profile, $l = 30 \mu$, solid curve, R versus I for $ZT_p/T_c = 10$, dashed curve, R versus I for anomalous dissipation and $\frac{v\Phi}{T_c} < 0.05$

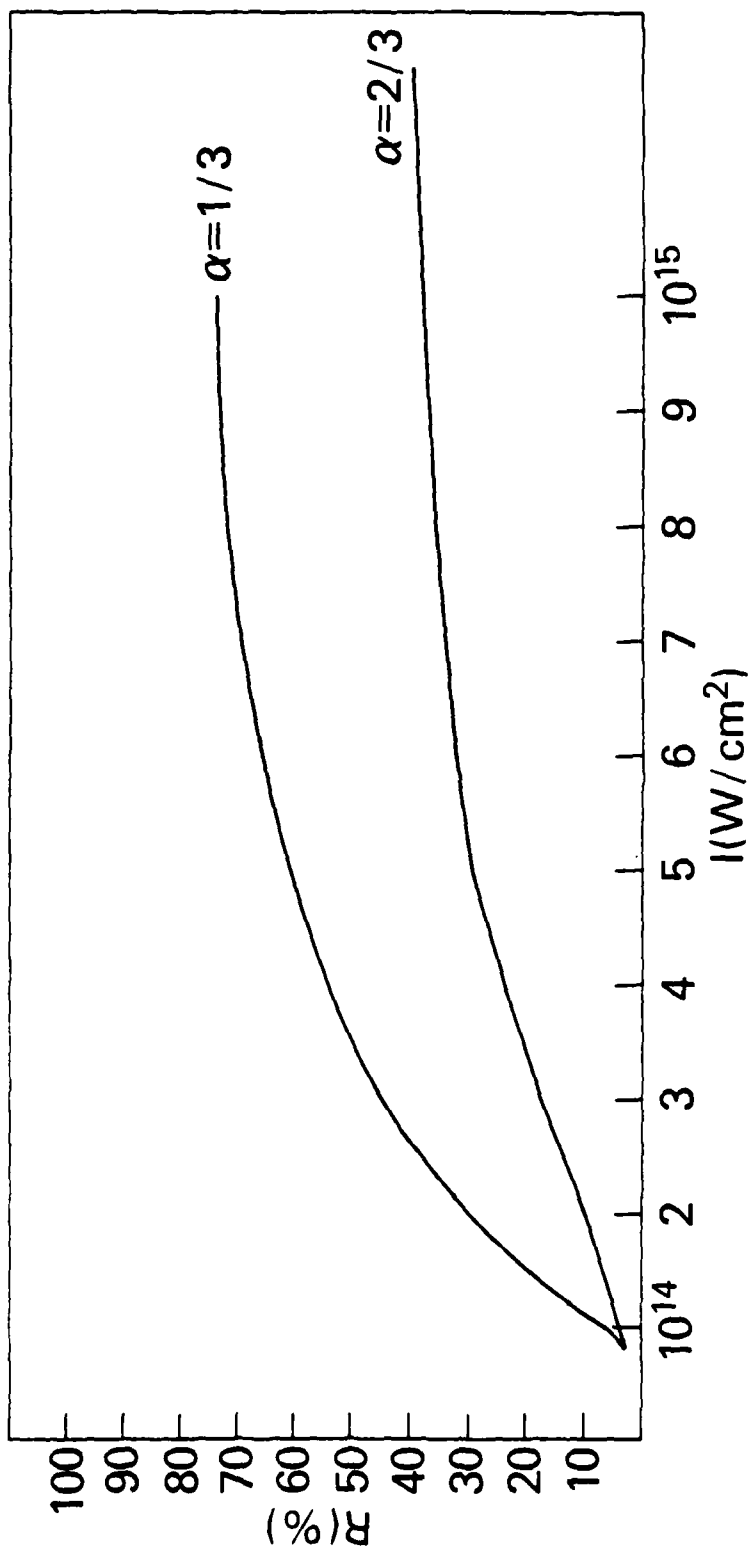


Fig 4 - Double structured density profile with $\nabla n = 0$, R versus I where $I_e = I^*$

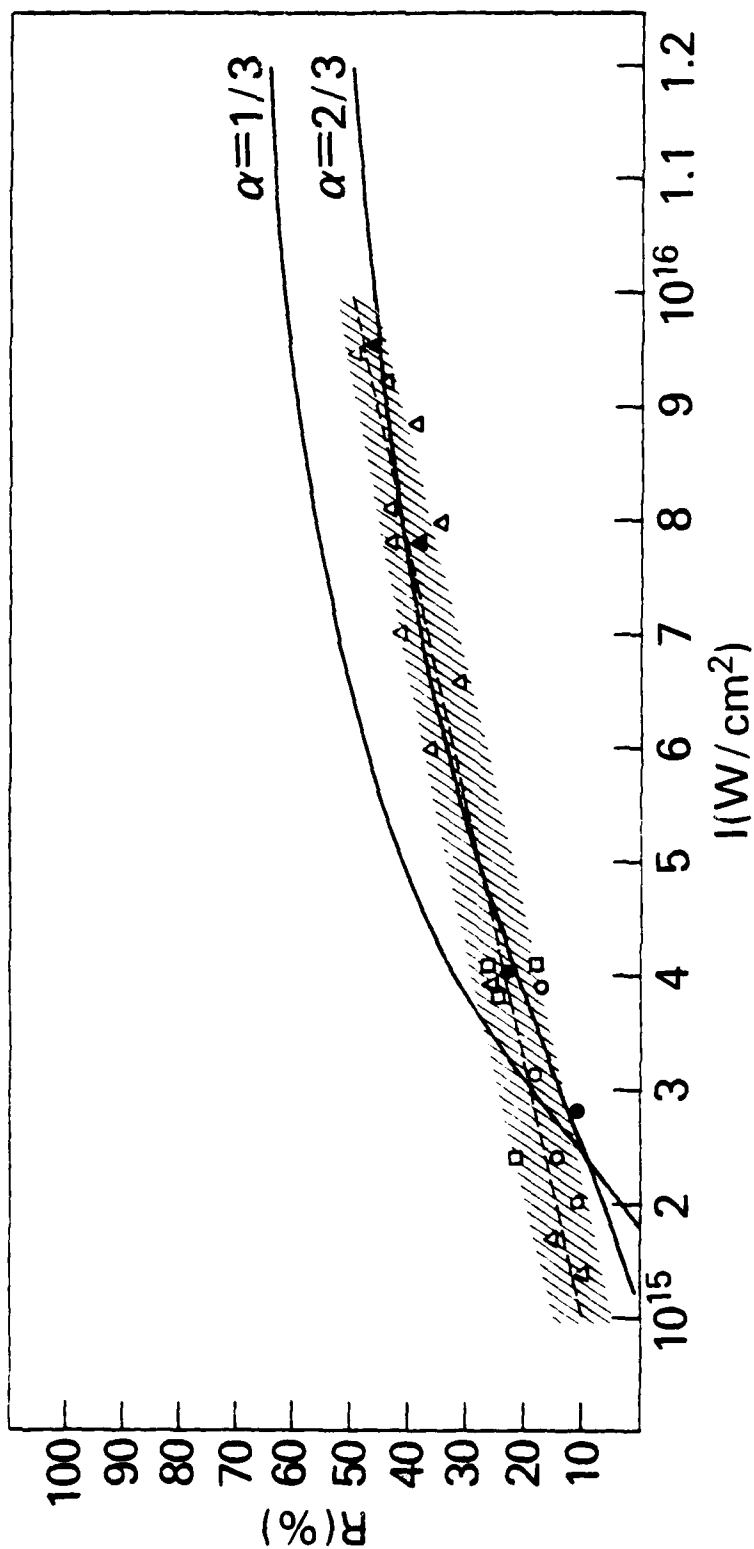


Fig. 5 — Double structured profile with $\chi_A \neq 0$, R versus I where $I_0 = I^*$. Also shown are the experimental points for Fig. 3 of Ref. 9.

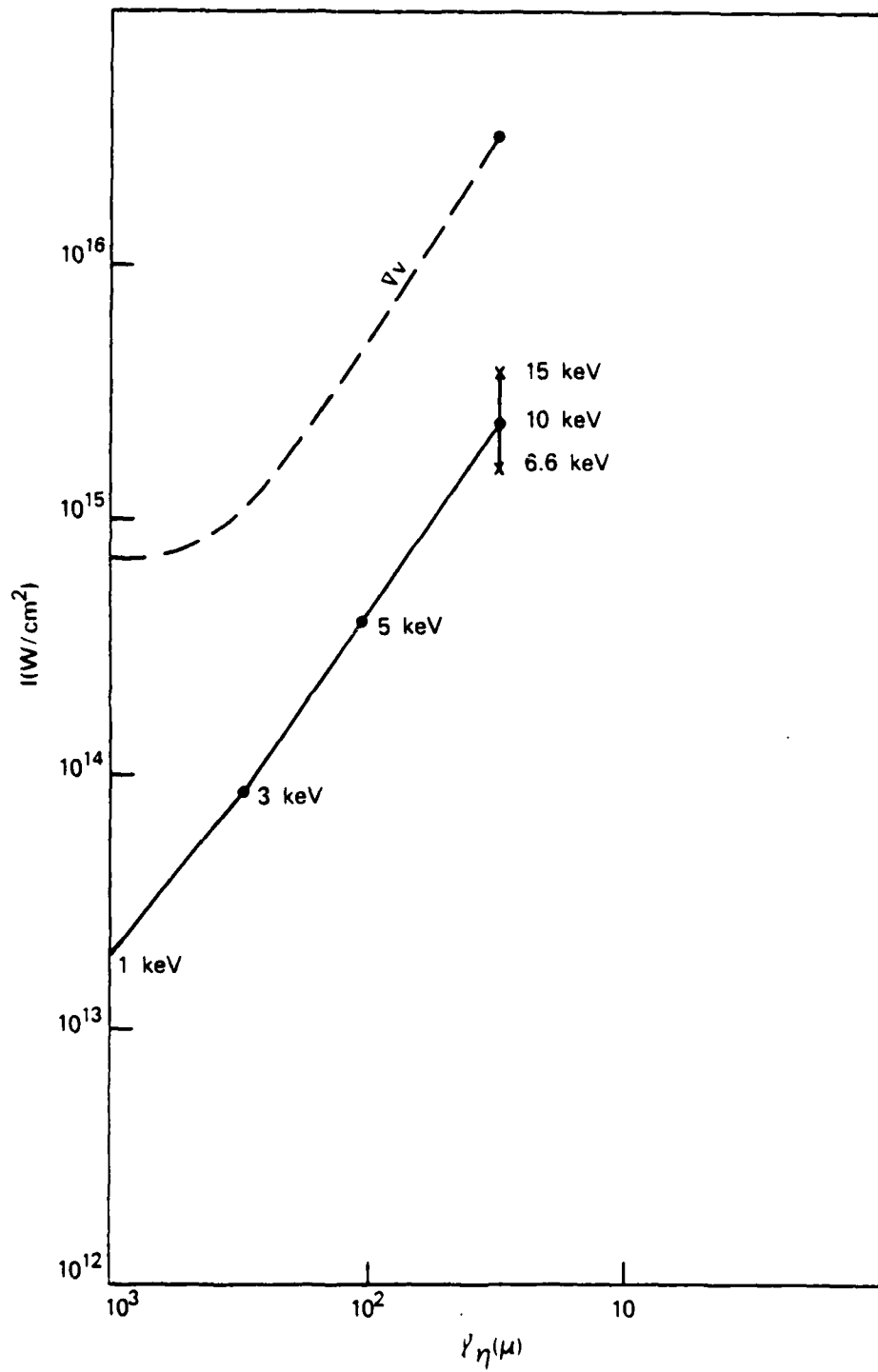


Fig. 5 - Irradiance for 50% reflection for a single structured pulse with and without velocity gradient as a function of scale length in microns

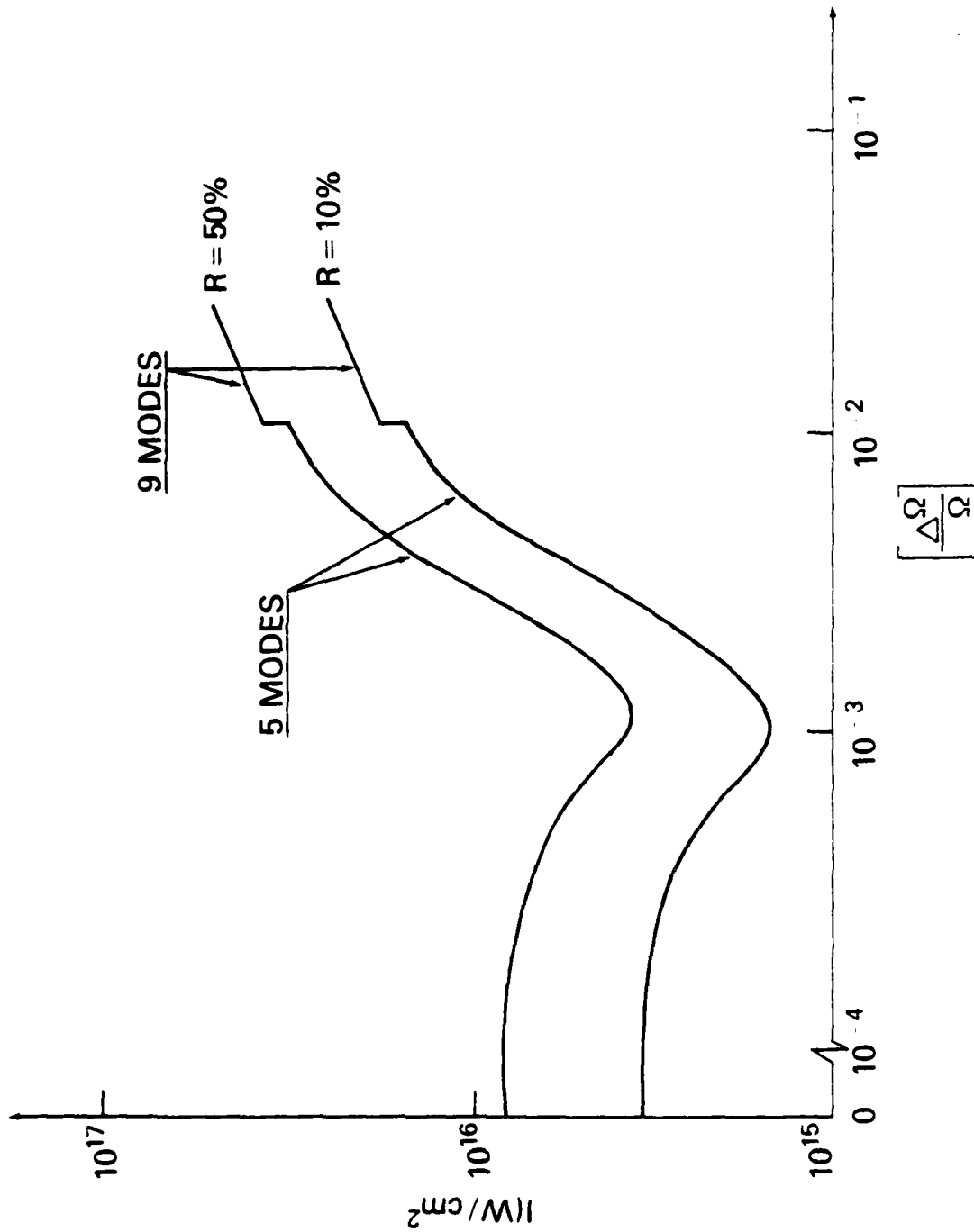


Fig. 7 - Irradiance for $R = 10\%$ and $R = 50\%$ as a function of $(\Delta\Omega/\Omega)$ for a wide band pump

DISTRIBUTION LIST

U.S.D.O.E. (50 copies)
P. O. Box 62
Oak Ridge, TN 37830

National Technical Information Service (24 copies)
U. S. Department of Commerce
5285 Port Royal Road
Springfield, VA 22161

NRL, Code 2628 (35 copies)
NRL, Code 4730 (50 copies)
NRL, Code 4790 (50 copies)
NRL, Code 4700 (25 copies)

U.S.D.O.E. (7 copies)
Office of Inertial Fusion
Washington, D.C. 20545
Attn: Dr. G. Canavan
Dr. R. Schriever
Dr. S. Kahalas
Dr. S. Barrich
Dr. T. Godlove
Dr. K. Gilbert

END

DATE
FILMED

5-8-11

DTIC